Solid-state NMR Characterization of Molecular Conformation in Disordered Methyl α–L–rhamnofuranoside.

James K. Harper,*[a] Derek Tishler,[b] David Richardson,[a] John Lokvam,[c] Robert Pendrill,[d] Göran Widmalm.[d]

[a]University of Central Florida, Department of Chemistry, 4000 Central Florida Blvd., Orlando, FL 32816, USA.
[b]University of Central Florida, Department of Physics, Orlando, FL 32816, USA.
[c]University of California Berkeley, Department of Biology, Berkeley, CA 94720, USA.
[d]Department of Organic Chemistry, Arrhenius Laboratory, Stockholm University, S-106 91, Stockholm, Sweden.

Solid-state NMR Characterization of Molecular Conformation in Disordered Methyl α–L–rhamnofuranoside.

Abstract.

A combination of solid-state ^{13}C NMR tensor data and DFT computational methods are utilized to predict conformation in disordered methyl α–L–rhamnofuranoside. This previously uncharacterized solid is found to be crystalline and consists of at least six distinct conformations that exchange on the kHz timescale. A total of 66 model structures were evaluated and six were identified as being consistent with experimental ^{13}C NMR data. All feasible structures have very similar heavy atom positions and differ most significantly in OH hydrogen orientations. A concerted rearrangement of OH hydrogens is proposed to account for the observed dynamic disorder. This rearrangement is accompanied by smaller changes in ring conformation and is slow enough to be observed on the NMR timescale due to severe steric crowding among ring substituents. The relatively minor heavy atom differences in the final structures suggest that characterization of a complete crystal structure by x-ray powder diffraction may be feasible.

Keywords. ^{13}C tensor principal values, NMR crystallography.

Introduction.

For the past century the insights provided by crystallography have help guide the development of science in a remarkably wide range of disciplines. Several well-established diffraction techniques are now available for determining structure in materials that form crystals and, to a lesser extent, microcrystalline powders. Recently, the methods of solid-state NMR have been directed toward the problem of crystallographic characterization and the prospect of performing "NMR crystallography" has become feasible.[1] Presently, most NMR crystallographic studies emphasize the NMR characterization of the molecular structure of an individual molecule or the repeating unit in framework materials.[2] The longer-range lattice order needed to identify a space group is usually obtained independently from x-ray powder diffraction methods that rely on the NMR determined structure as a starting model. However, alternative methods[3] including theoretical crystal structure prediction methods have also been found to be capable of also providing the lattice structure.[2b,4]

Crystallographic analysis by NMR spectroscopy is appealing because NMR is capable of characterizing a diverse variety of solids that can be difficult to treat by conventional diffraction methods. A key early development in the pursuit of crystal structure by NMR was the ability to characterize molecular conformation by solid-state NMR.[5] Such structural characterizations can now be achieved using a variety of methods and have been used to elucidate structure in proteins,[6] inorganic materials[2a,2b,2h,2i,2l,2m] and smaller organic molecules.[7] Presently, these studies have largely been limited to well-ordered crystalline solids and extension to more challenging materials is desirable. For example, many materials form solids containing molecules that are partially disordered or

that consist of mixtures of several lattice types (i.e. mixed phase materials). In these cases NMR has the potential to provide molecular conformation for each unique structure found in the solid because several resonances are usually observed for each atomic position due to the multiple distinct conformations present in the solid.

Solid-state NMR is remarkably sensitive to even minor differences in structure and such variations, when present, often result in new resonances for a given site. Thus, disordered or mixed phase solids usually exhibit several resonances for each atom in the molecule. Conformational characterization for each unique structure in these solids is valuable because such structures provide the initial models needed for crystal structure determination by powder diffraction methods. Accordingly, the aim of the present study is to characterize the molecular conformations of one such disordered solid, namely, methyl α–L–rhamnofuranoside (Figure 1). Presently, there is no known crystal structure for methyl α–L–rhamnofuranoside and this study will provide the structure of the crystallographic asymmetric unit for each conformation present. Inspection of the ^{13}C NMR spectrum of solid methyl α–L–rhamnofuranoside shows disorder at several of the carbons and narrow lines characteristic of a crystalline solid. Here, ^{13}C tensor principal values are measured for all sites. Assignment of conformation is accomplished using a previously described approach[5a] that evaluates a wide variety of possible conformations and retains structures having computed tensors that agree with experimental data.

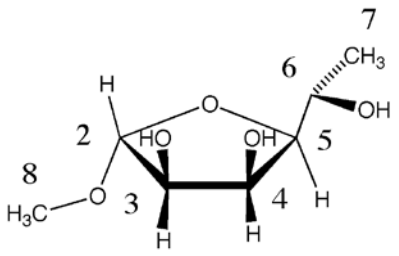

Figure 1. Schematic of methyl α–L–rhamnofuranoside including the numbering used herein.

Experimental and Theoretical Methods.

Methyl α-L-rhamnofuranoside was synthesized by dissolving L-rhamnose (5.00 g, 30.5 mmol) in MeOH (15 mL) and adding Dowex-50 (H^+ form). The mixture was kept at reflux for 2 h and then left to cool. After filtering, the solvent was evaporated under reduced pressure, leaving a sticky residue that was purified by flash chromatography with gradient elution (50% → 0% toluene in EtOAc followed by 10% MeOH in EtOAc). Fractions containing the earliest eluting product were pooled and evaporated under reduced pressure, yielding the title product (477 mg, 2.67 mmol, 8.8%) which upon recrystallization from Et_2O gave clear needles (87 mg, 0.5 mmol, 1.6%). ^{1}H NMR recorded on a Bruker Avance 400 MHz spectrometer equipped with a 5 mm BBO probe in D_2O at ambient temperature reported in ppm and referenced to internal sodium 3-trimethylsilyl-(2,2,3,3-$^2H_4$)-propanoate (δ_H 0.00): δ_H 1.29 (d, 3H, J = 6.3 Hz, H7), 3.47 (s, 3H, H8), 3.90 (dd, 1H, J = 8.1, 3.0 Hz, H5), 4.04 (dq, 1H, J = 8.1, 6.3 Hz, H6), 4.15 (dd, 1H, J = 4.6, 4.6 Hz, H3), 4.33 (dd, 1H, J = 4.6, 3.0 Hz, H4), 4.96 (d, 1H, J = 4.6 Hz, H2). ^{13}C NMR in D_2O at ambient temperature reported in ppm and referenced to external 1,4-dioxane in D_2O (δ_C 67.40): δ_C 19.9 (C7), 57.0 (C8), 65.7 (C6), 71.8 (C4), 77.5 (C3), 84.3 (C5), 109.2 (C2).

Double-quantum filtered COSY data was acquired on a Varain 500 MHZ INOVA spectrometer using a 5 mm probe and approximately 37 mg of methyl α-L-rhamnofuranoside dissolved in 0.7 mL of CD_3OD. A ^1H 90° pulse width of 5.55 μs was used together with a recycle time of 1 s and F1 and F2 spectral widths of 2.34 kHz. A total of 256 evolution increments of 8 scans each were acquired. Total acquisition time was 1.5 h.

All solid-state 1D ^{13}C spectra were acquired on a Chemagnetics CMX400 spectrometer using a 7.5 mm probe. Operating conditions included a spectral width of 13.228 kHz, a ^{13}C operating frequency of 100.615993 MHz, a ^1H decoupling frequency of 400.11960 MHz, a ^1H 90° pulse width of 3.9 μs and a cross polarization time of 3.0 ms. Proton decoupling employed the TPPM sequence[8] with a ^1H 180° pulse of 8.1 μs and a phase angle difference of 8° between adjacent pulses. A pulse delay of 7.0 s was used and the digital resolution was 12.9 Hz/point for all spectra. Data were acquired at spinning speeds of 2.3 kHz, 3.0 kHz, 4.0 kHz and 4.8 kHz. All spectra were externally referenced to the methyl resonance of hexamethyl benzene at 17.35 ppm.

The FIREMAT[16] data was acquired at a spinning speed of 575 Hz using evolution and acquisition spectral widths of 13.227 and 72.464 kHz, respectively. A total of 23 evolution increments of 768 scans each were acquired. All other acquisition parameters were identical to those used for 1D ^{13}C data acquisition. The final data was rearranged and processed according to a scheme described elsewhere.[16] A digital resolution of 17.7 Hz per point was obtained in the acquisition dimension. An evolution dimension digital resolution of 17.7 Hz per point was obtained after the data rearrangement.

The conformational analysis considered only staggered structures since such

conformations are nearly always found in diffraction structures of related carbohydrates. Because the chemical shift is influenced primarily by local structure,[9] it is possible to further simplify the conformational analysis by initially considering molecular sites that are somewhat isolated from other flexible moieties. In practice, an isolated site is one that is at least three bonds removed from any other flexible moiety.[9] More distant sites are allowed to assume arbitrary conformations since they are too far removed to influence the site of interest. This process has been used previously[5d,7b] and allows a stepwise determination of structure that significantly reduces the number of conformations that must be considered. Accordingly, initial conformational analysis focused solely on rotations about the C2–OCH_3 bond since the methyl can be considered to be isolated. Three staggered conformation about the C2–OCH_3 bond were prepared and relaxed using Gaussian at the B3LYP/D95* level of theory.[10] The bulky methoxy group was found to always reorient to a position with the methoxy group oriented as shown in Figure 7 (see below) regardless of the initial starting position. Of equal importance, the C2 ^{13}C tensor data computed using this conformation was found to agree well with experimental data. Thus, only this C2–OCH_3 conformation was considered in subsequent calculations. Selection of best fit conformations at C3–O involved creation of all combinations of staggered conformations about C3–O and the only neighboring site, C4–O (9 total), relaxing each structure and comparing computing ^{13}C tensor principal values with experimental data. One conformation at C3 was eliminated by this comparison. To further establish conformations, all combinations of conformations about C4–O, C5–C6 and C6–O had to be considered because none can be considered isolated from the other sites. A total of 27 structures are possible and each was prepared and relaxed. Since

each of these structures had to be combined with one of the two possible orientations at C3–O, a total of 54 structures were evaluated. Overall, this process required consideration of 66 conformations rather than the 243 structures that would have been evaluated if isolated regions had not been utilized. A total of 20 structures failed to converge due to steric crowding that could not be alleviated. The remaining structures converged based on energy considerations and all structures were found to lie within 26.4 kJ mol^{-1} of the lowest energy structure. NMR shift tensors were calculated for all energetically feasible structures at the B3PW91/D95** level of theory.[10a,11] This theoretical treatment was chosen because the error in computed tensor data is known from previous work to be 1.79 ppm.[4] A comparison of these computed NMR data to the experimental shift tensor data revealed that six of the model structures agreed with experimental data. All tensor comparisons were done in the icosahedral representation[12] to allow equal weighting of all data points. Two figures of merit were used to compare calculated and experimental tensor data. First, the fit at all positions was considered and feasible structures selected according to a method described elsewhere.[13] This comparison eliminated all but 15 of the model structures. A second comparison removed any structure having an unacceptably large error in *any* principal value. Here large errors were defined as errors larger than three times the expected error (i.e. roughly 6 ppm). This second standard eliminated all but the 6 structures illustrated in Figures 5 & 6 (see below).

Results and discussion.

Characterizing disorder.

Methyl α–L–rhamnofuranoside is typical of solids that contain disorder with multiple ^{13}C resonances observed for atoms in the molecule (Figure 2). Such NMR spectra can arise from either static or dynamic disorder of the individual molecules. Many of the features observed in spectra of disordered solids are also seen in solids containing two or more molecules in the crystallographic asymmetric unit (i.e. Z' > 1). Fortunately, solids with Z' > 1 can usually be distinguished from disordered materials since they contain resonances that are relatively insensitive to temperature variations and that occur in approximately 1:1 ratios. The methyl α–L–rhamnofuranoside studied here has a ^{13}C spectrum characteristic of a disordered solid.

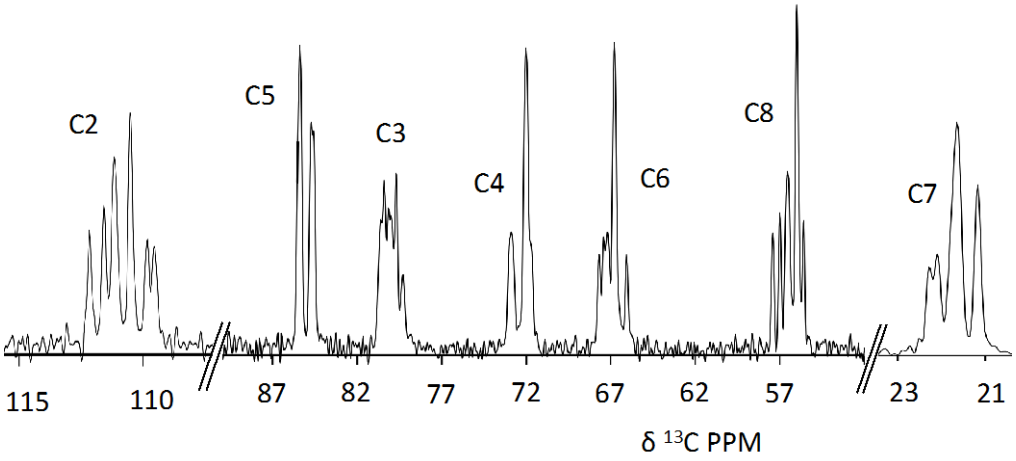

Figure 2. The ^{13}C CP/MAS spectrum of methyl α–L–rhamnofuranoside. Each atomic position displays multiple resonances, reflecting the dynamic disorder present in the powder. As many as six resonances are observed for each carbon, indicating the presence of six rapidly interconverting conformations in the solid. Regions of the spectrum containing no resonances have been omitted.

A series of 1D ^{13}C spectra were collected to determine whether the disorder in methyl α–L–rhamnofuranoside is static or dynamic. The disorder was found to be dynamic based upon spectra acquired over a range of spinning speeds from 2.3 - 4.8 kHz (Figure 3). In these experiments, the number of resonances per position was found to vary with spinning speed. These changes were reproducible at all spinning speeds regardless of sample spinning history, eliminating the possibility that the changes in chemical shift were caused by a pressure induced phase change. This result is consistent with conformational exchanges that occur at rates comparable to the spinning speed with significant differences observed at C2, C3, C4, and C8. To create the observed changes in the spectrum, the exchange must occur within the rotor period to alter the rotor echo. Thus, in the methyl α–L–rhamnofuranoside phase studied here, conformational exchange at C2, C3, C4, and C8 occurs in the kHz range. No effort was made to more accurately quantify dynamics since the focus of the present study was to determine which conformations are present in the solid and to evaluate the magnitude of the conformational differences.

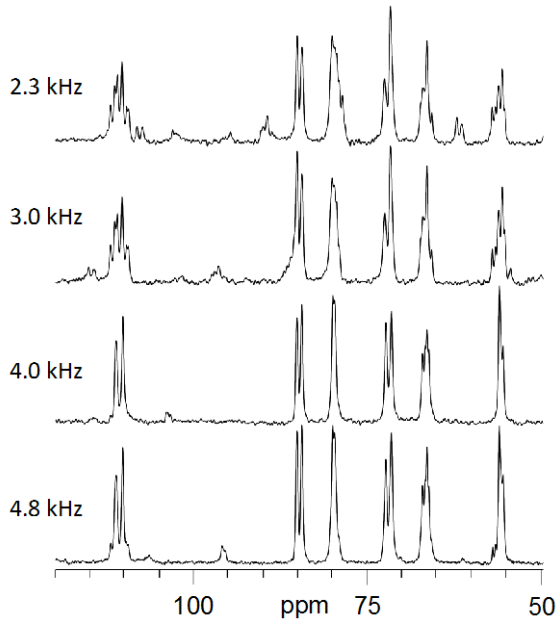

Figure 3. A comparison of ^{13}C CP/MAS spectra of methyl α–L–rhamnofuranoside acquired at four spinning speeds. The changes in the spectra are consistent with dynamic disorder in the kHz range. The C7 methyl resonance is omitted to allow splitting at other frequencies to be more clearly observed.

Assignment of ^{1}H and ^{13}C chemical shifts.

Accurate structural studies require that all chemical shifts be correctly assigned to the corresponding nuclei. The ^{1}H and ^{13}C shift assignments of methyl α–L–rhamnofuranoside in solution have been reported previously.[14] Since these assignments were based exclusively on 1D data, new solution phase analyses were performed to verify all assignments. These new data were conducted in CD_3OD and rely primarily on DQF-COSY data (see experimental). All assignments reported previously were found to be correct and only minor changes in frequency were observed in CD_3OD. All assignments and important DQF-COSY correlations are listed in Table 1.

Table 1. Proton and ^{13}C chemical shift assignments (ppm) for methyl α–L–rhamnofuranoside.

	D_2O[a]		CD_3OD		DQF-COSY
position	^1H	^{13}C	^1H	^{13}C	$^1H \rightarrow {}^1H$ correlations
2	4.96 (4.94)	109.2 (109.7)	4.80	110.20	4.80 → 3.99
3	4.15 (4.12)	77.5 (77.8)	3.99	78.35	3.99 → 4.80 & 4.27
4	4.33 (4.31)	71.8 (72.3)	4.27	72.64	4.27 → 3.99 & 3.69
5	3.90 (3.85)	84.3 (84.7)	3.69	84.70	3.69 → 4.27 & 4.02
6	4.04 (4.03)	65.7 (66.4)	4.02	66.91	4.02 → 3.69 & 1.25
7	1.29 (1.28)	19.9 (20.4)	1.25	20.51	1.25 → 4.02
8	3.47 (3.45)	57.0 (57.2)	3.36	55.98	–

[a]Chemical shifts shown in parentheses are those reported previously.[14] All other chemical shifts in D_2O were independently acquired in the present study to verify the stereochemistry of the material evaluated herein.

All chemical shift assignments in solid methyl α–L–rhamnofuranoside were made by comparison to those in solution. A comparison of tensor principal values (described below) shows a close agreement between all experimental and calculated chemical shifts, further validating the assignments shown.

Conformational predictions.

Prior work has demonstrated that accurate conformations can be predicted from ^{13}C chemical shift tensor information.[15] Accordingly, tensor data was collected for methyl α–L–rhamnofuranoside using the FIREMAT[16] experiment. All tensor values are listed in Table 2. At a spinning speed of 2.3 kHz up to six resonances per position were observed indicating the presence of six distinct conformations present in rapid exchange. Slower spinning did not alter the spectrum, thus the FIREMAT analysis was acquired at 575 Hz to yield the maximum number of resonances per position while simultaneously allowing a large number of sidebands to be observed for each tensor powder pattern. A

sample of the resolution and signal-to-noise obtained from the FIREMAT analysis is shown in Figure 4.

Table 2. The ^{13}C principal value chemical shifts (ppm) for solid methyl α–L–rhamnofuranoside.

position	δ_{11}	δ_{22}	δ_{33}	δ_{iso}
C2	127.5	101.7	99.4	109.5
	127.6	101.0	101.0	109.8
	127.7	104.0	99.8	110.5
	128.1	105.9	99.4	111.1
	129.1	106.2	99.5	111.6
	129.3	107.2	100.0	112.2
C3	104.5	77.4	55.9	79.3
	103.5	78.2	57.3	79.7
	103.2	80.1	56.6	80.0
	102.2	80.0	58.1	80.1
	103.4	79.2	58.6	80.4
	104.8	78.1	59.1	80.7
C4	96.2	67.9	51.2	71.7
	94.8	68.7	52.7	72.0
	95.1	70.4	53.3	72.9
C5	117.0	82.2	54.6	84.6
	115.6	82.7	56.1	84.8
	120.5	81.5	54.4	85.5
C6	87.9	81.2	29.1	66.1
	89.4	82.3	28.6	66.8
	87.6	84.1	29.9	67.2
	89.7	83.7	28.9	67.4
	91.0	83.7	28.5	67.7
C7	33.7	27.4	2.5	21.2
	33.3	29.1	2.4	21.6
	31.3	31.2	2.8	21.8
	34.9	27.7	3.7	22.1
	31.3	31.3	4.4	22.3
C8	85.3	73.5	7.9	55.6
	87.3	74.2	6.2	55.9
	86.7	75.4	5.9	56.0
	86.7	73.9	8.9	56.5
	87.4	76.8	6.8	57.0
	87.8	74.2	10.4	57.4

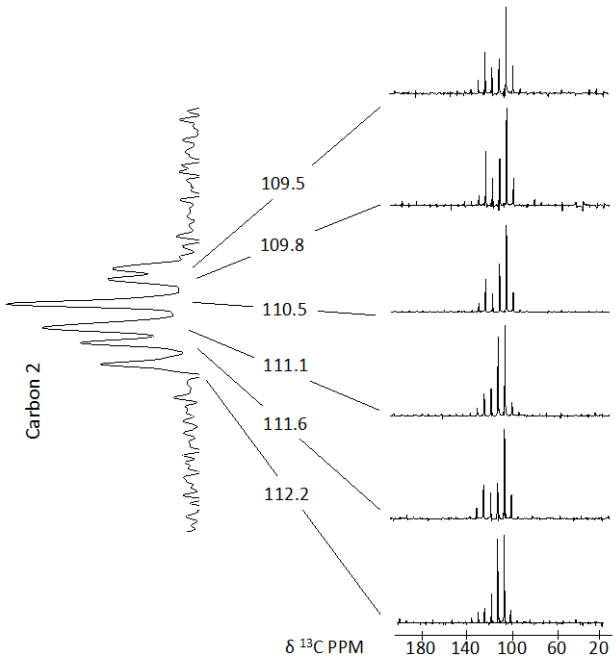

Figure 4. The FIREMAT data from carbon 2 illustrating the high resolution and signal-to-noise data obtained from the analysis. All other positions provided comparable high quality data.

A total of 243 conformations are possible if only staggered conformations about the C2–OCH_3, C3–O, C4–O, C5–C6, and C6–O bonds are considered. Only staggered conformations were evaluated because such conformations, or small deviations from these conformations, are invariably found in diffraction structures of related carbohydrates. Calculation of relaxed geometry and ^{13}C principal values for all 243 conformations was considered impractical and thus a previously described process[5d] was employed that allows significantly fewer structures to be considered while retaining accuracy. Overall, a total of 66 conformational models were considered and each of these was evaluated to identify energetically favorable structures. A more detailed description of how structures were selected and the relaxation of initial model structures

is included in Experimental Methods. Tensors were computed for each of the optimized structures and those agreeing with experimental tensor data were retained as viable conformations. It is now possible to include lattice fields in theoretical tensor computations. However, in the case of carbohydrates, it has been demonstrated that inclusion of such lattice fields corrects the calculations by less than 1 ppm.[17] In contrast, conformational variations due to the rotation of a single OH hydrogen are known to cause changes in ^{13}C principal values as large as 10 ppm.[18] Moreover, the error in experimental ^{13}C principal values from FIREMAT is roughly 1 ppm.[2k] Thus, for carbohydrates, use of gas phase calculations introduces a negligible error much smaller than the changes due to conformational variations. Accordingly, gas phase calculations were used for all structural predictions described herein.

In disordered samples, comparison between experimental and calculated tensor shift values is challenging because multiple resonances are observed for each ^{13}C site in the molecule and identifying one particular set of lines arising from a single conformation can be difficult. Assigning all lines to individual conformations has been accomplished by van Rossum[19] and others[20] using $^{1}H/^{13}C$ correlation data. However, in methyl α–L–rhamnofuranoside most experimental principal values from a given position in the molecule show only minor differences of ca. ± 1 ppm. Errors in calculated ^{13}C tensor data for similar carbohydrates are known from prior work to be roughly 1.8 ppm.[4] Thus, most of the experimental values for a given position display differences less than the error in the calculated values. Accordingly, principal values for many positions were averaged for comparison purposes. This approach recognizes that experimental principal values having differences smaller that the error in calculated shifts will inevitably be

assigned to the same conformation. Nevertheless, some differences in experimental chemical shifts larger than the error in calculated values were observed at C2 (δ_{22}), C5 (δ_{11}), and C8 (δ_{33}). At these sites, two populations of principal values could be distinguishable. All averaged experimental data used for conformational predictions is summarized in Table 3.

Table 3. The averaged ^{13}C NMR shift tensor principal values used for comparison with calculated model structures.

position		tensor principal values (ppm)	
C2	δ_{11}	128.6 ± 0.8	127.6 ± 0.1
	δ_{22}	105.8 ± 1.3	101.5 ± 0.5
	δ_{33}	99.7 ± 0.3	100.2 ± 1.1
C3	δ_{11}	103.6 ± 0.9	
	δ_{22}	78.8 ± 1.1	
	δ_{33}	57.6 ± 1.2	
C4	δ_{11}	95.4 ± 0.7	
	δ_{22}	69.0 ± 1.3	
	δ_{33}	52.4 ± 1.1	
C5	δ_{11}	116.3 ± 1.0	120.5[a]
	δ_{22}	82.4 ± 0.4	81.5[a]
	δ_{33}	55.4 ± 1.1	54.4[a]
C6	δ_{11}	89.1 ± 1.4	
	δ_{22}	83.0 ± 1.2	
	δ_{33}	29.0 ± 0.6	
C7	δ_{11}	32.9 ± 1.6	
	δ_{22}	29.3 ± 1.9	
	δ_{33}	3.2 ± 0.9	
C8	δ_{11}	86.6 ± 1.3	87.1 ± 0.4
	δ_{22}	73.9 ± 0.4	75.5 ± 1.3
	δ_{33}	9.1 ± 1.3	6.3 ± 0.5

[a]Only a single isotropic resonance at 85.5 ppm had principal values with the higher frequency δ_{11} component shown. Accordingly, no standard deviation was obtained for this resonance.

A total of eight unique combinations of experimental principal values can be made from the data from table 3. When each of these experimental datasets was

compared to the model structures, six conformations were found to be compatible with the experimental data. All other models were rejected with > 90% confidence. The selected conformations are shown superimposed in Figure 5 with only heavy atom positions displayed. Differences showing both hydrogens and heavy atoms positions are shown in Figure 6. It is noteworthy that rapid dynamics would be expected to reduce the span of the chemical shift tensor (i.e. $\delta_{11} - \delta_{33}$). The fact that experimental and computed spans closely match at all positions independently confirms that the exchange is slow on NMR timescale.

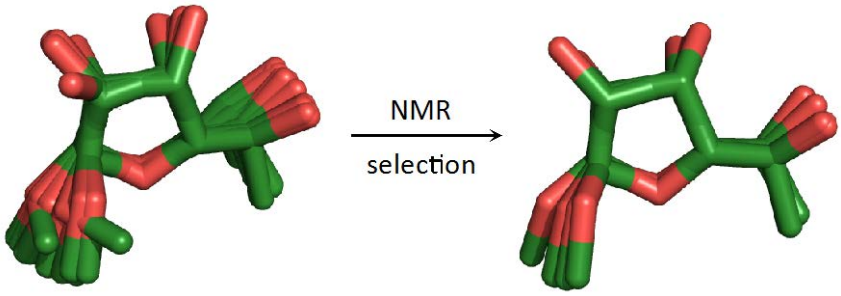

Figure 5. A wide variety of molecular conformations were initially evaluated (left). Of these, six structures (right) were found to be compatible with all ^{13}C shift tensor principal values data.

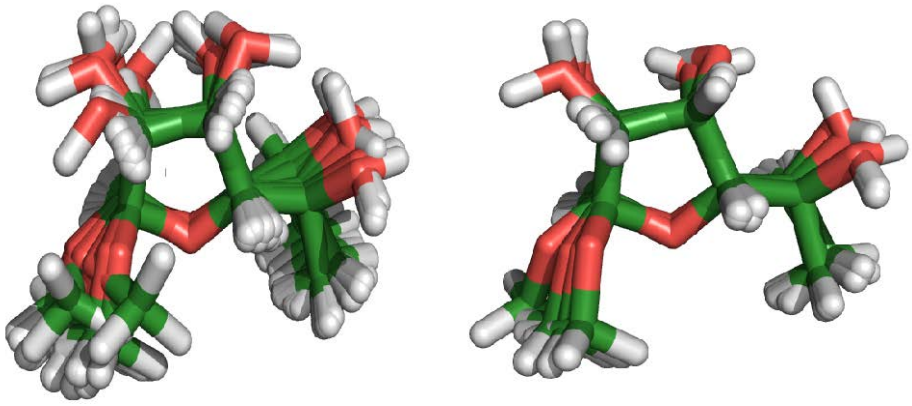

Figure 6. All conformations of methyl α–L–rhamnofuranoside evaluated are shown with hydrogen atoms included in the left figure. Those conformations consistent with the ^{13}C chemical shift tensor data are shown at the right. The structures retained as feasible (right) can be seen to differ most significantly in OH hydrogen positions and are thought to interconvert via a concerted OH reorientation.

The six structures agreeing with the ^{13}C shift tensor data were analyzed in detail. All degrees of freedom are reported in Table 4. The flexibility is largely described by four ring conformations; $^{3}T_{4}$, $^{5}T_{O}$, ^{5}E and E_{O}, described quantitatively by their respective Cremer-Pople puckering parameters.[21] For the O5-C2-O8-C8 and O5-C5-C6-O6 dihedral angles, all models have similar conformations, with approximately –65° for the former and approximately 180° for the latter.

Table 4. Conformational descriptors of the six model structures agreeing with ^{13}C chemical shift tensor principal values.

model no.	ring conf.	q_2	φ_2 (°)	O5-C2-O8-C8 (°)	O5-C5-C6-O6 (°)	H-C-O-H (°) 3	4	6
23	^{5}E	0.375	136.8	-66.6	183.8	36.7	-109.2	190.9
24	^{5}E	0.374	137.9	-66.0	185.1	36.4	-110.4	311.0
26	$^{3}T_{4}$	0.385	85.2	-70.6	165.2	-59.3	56.7	189.4
27	$^{3}T_{4}$	0.385	85.4	-70.4	166.2	-58.9	57.2	285.8
35	$^{5}T_{O}$	0.383	156.3	-66.2	184.8	58.7	-147.9	190.2
36	E_{O}	0.332	184.9	-63.9	169.5	40.3	-152.8	50.9

The hydroxyl torsions have roughly staggered conformations and for the hydroxyl

groups at carbons 3 and 4, essentially the same values are found for each ring conformation. The only degree of freedom that shows different conformations with maintained ring conformation is the hydroxyl torsion at position 6, which shows two different values for the $^{3}T_{4}$ and the ^{5}E ring conformations, hence giving rise to the two additional structures needed to explain the six different sets of ^{13}C shift tensors. Figure 7 provides a visual comparison of structures described in Table 4.

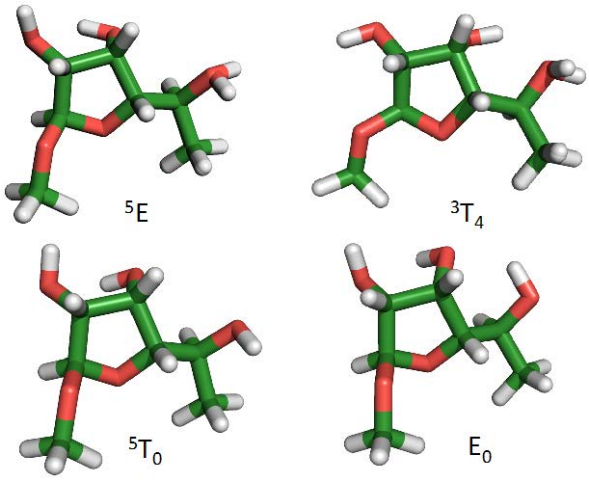

Figure 7. A comparison of the four ring conformations found to agree with ^{13}C tensor principal value data. The ^{5}E and $^{3}T_{4}$ structures consist of two superimposed conformations that differ primarily in the OH orientation at C6.

The hydroxyl group at position 4 is acting as a hydrogen bond donor in all of the model structures, with either O3 or O6 as the acceptor (Table 5). In the E_O conformation two hydrogen bonds are formed, creating the hydrogen bond chain O6–H···O4–H···O3. However, it is anticipated that if hydroxyl groups as donors were to be refined in an X-ray crystallographic analysis, intermolecular hydrogen bond networks would also be found, since the O_{donor}–H···$O_{acceptor}$ interactions identified here all have angles < 135°,

which is the lower limit commonly used to identify hydrogen bonds by geometric criteria.

Table 5. Hydrogen bonds found in the six model structures agreeing with ^{13}C NMR tensor data.

model no.	hydrogen bond	$r_{OH\cdots O}$ (Å)	$\angle_{O-H\cdots O}$ (°)
23	O4H···O3	2.0	123.2
24	O4H···O3	2.0	123.5
26	O4H···O6	2.2	126.1
27	O4H···O6	2.2	125.9
35	O4H···O3	2.1	111.5
36	O4H···O3	2.0	114.9
	O6H···O4	2.1	131.3

The structures selected show that the disorder in methyl α–L–rhamnofuranoside consists primarily of disorder in hydrogen positions. This disorder most likely consists of a dynamic reordering in hydrogen bonding in which the OH hydrogens rearrange on the kHz timescale to form new conformations that are nearly isoenergetic. This process is well known in other carbohydrates in the solid state[22] but usually occurs at rates of 10^{11} – 10^{16} jumps per second, allowing only averaged resonances to be observed by SSNMR. In the case of methyl α–L–rhamnofuranoside, this process is much slower and allows distinct resonances from the individual contributing structures to be observed. One possible explanation for this slower reorientation is that methyl α–L–rhamnofuranoside has severe steric crowding. Thus, any rearrangement of an OH hydrogen would require a concerted rearrangement in adjacent OH positions. The concerted reordering of several positions in the molecule would likely be a slower process than a simple rotation of a single hydroxyl.

In contrast to the large hydrogen disorder, the heavier atom positions show only minor disorder as illustrated by the structures shown in Figure 5. This observation is consistent with minor heavy atom rearrangements from changes in ring conformations

that accompany the OH reorientations. The disorder in non-hydrogen sites is comparable to the thermal disorder observed in many single crystal x-ray diffraction structures and we therefore consider methyl α–L–rhamnofuranoside to be a good candidate for structural characterization by x-ray powder methods. The present study gives a detailed structural description of the crystallographic asymmetric unit and provides the initial model needed for a complete crystal structure determination.

Conclusions.

In this study, solid-state NMR ^{13}C tensor data are paired with computational methods to establish molecular conformation in a small carbohydrate that is dynamically disordered in the solid state and unsuitable for conventional single crystal diffraction techniques. The solid consists of at least six conformations that interconvert on the kHz timescale. An evaluation of dozens of candidate structures by computational methods identifies six conformations that are consistent with the NMR data. These structures differ primarily at OH hydrogen positions with heavier atoms exhibiting only minor differences that appear to arise from changes in ring conformation that accompany the OH hydrogen reorientations. This study serves to define the structure in the crystallographic asymmetric unit and to identify favorable intramolecular hydrogen bonding arrangements.

Supporting Information.

Coordinates for the six conformations of methyl α–L–rhamnofuranoside found to be consistent with ^{13}C NMR shift tensor data. This material is available free of charge via the internet at http://pubs.acs.org.

References.

1. Harris, R. K. *NMR Crystallography*; Wiley: Chichester, 2009.

2. (a) Brouwer, D. H.; Darton, R. J.; Morris, R. E.; Levitt, M. H. A Solid-State NMR Method for Solution of Zeolite Crystal Structures. *J. Am. Chem. Soc.* **2005**, *127*, 10365-10370. (b) Dutour, J.; Guillou, N.; Huguenard, C.; Taulelle, F.; Mellot-Draznieks, C.; Fe´rey, G. Chiolite, a Case Study for Combining NMR Crystallography, Diffraction and Structural Simulation. *Solid State Sci.* **2004**, *6*, 1059-1067. (c) Rajeswaren, M.; Blanton, T. N.; Zumbulyadis, N.; Giesen, D. J.; Conesa-Moratilla, C.; Misture, S. T.; Stephens, P. W.; Huq, A. Three-Dimensional Structure Determination of N-(p-tolyl)-dodecylsulfonamide from Powder Diffraction Data and Validation of Structure Using Solid-State NMR Spectroscopy. *J. Am. Chem. Soc.* **2002**, *124*, 14450-14459. (d) Middleton, D. A.; Peng, X.; Saunders, D.; Shankland, K.; David, W. I. F.; Markvardsen, A. Conformational Analysis by Solid-State NMR and its Application to Restrained Structure Determination from Powder Diffraction Data. *J. Chem. Commun.* **2002**, 1976-1977. (e) Harper, J. K.; Grant, D. M.; Zhang, Y.; Lee, P. L.; Von Dreele, R. Characterizing Challenging Microcrystalline Solids with Solid State NMR Shift Tensor and Synchrotron and X-ray Powder Diffraction Data: Structural Analysis of Ambuic Acid. *J. Am. Chem. Soc.* **2006**, *128*, 1547-1552. (f) Harris, R. K.; Ghi, P. Y.; Hammond, R. B.; Ma, C. Y.; Roberts, K. J.; Yates, J. R.; Pickard, C. Solid-State NMR and Computational Studies of 4-Methyl-2-nitoracetanalide. *J. Magn. Reson. Chem.* **2006**, *44*, 325-333. (g) Smith, E. D. L.; Hammond, R. B.; Jones, M. J.; Roberts, K. J.; Mitchell, J. B. O.; Price, S. L.; Harris, R. K.; Apperley, D. C.;

Cherryman, J. C.; Docherty, R. The determination of the Crystal Structure of Anhydrous Theophylline by X-ray Powder Diffraction with a Systematic Search Algorithm, Lattice Energy Calculations and ^{13}C and ^{15}N Solid-State NMR: A Question of Polymorphism in a Given Unit Cell. *J. Chem. Phys. B* **2001**, *105*, 5818-5826. (h) Brouwer, D. H. NMR Crystallography of Zeolites: Refinement of an NMR-Solved Crystal Structure Using ab Initio Calculations of ^{29}Si Chemical Shift Tensors. *J. Am. Chem. Soc.* **2008**, *130*, 6306-6307. (i) King, I. J.; Fayon, F.; Massiot, D.; Harris, R. K.; Evans, J. S. O. A Space Group Assignment of ZrP_2O_7 Obtained by ^{31}P Solid State NMR. *Chem. Commun.* **2001**, 1766-1767. (j) Witter, R.; Sternberg, U.; Hesse, S.; Kondo, T.; Koch, F. T.; Ulrich, A. S. ^{13}C Chemical Shift Constrained Crystal Structure Refinement of Cellulose I_α and its verification by NMR Anisotropy Experiments. *Macromolecules* **2006**, *39*, 6125-6132. (k) Harper, J. K.; Doebbler, J. A.; Jacques, E.; Grant, D. M.; Von Dreele, R. B. A combined Solid-State NMR and Synchrotron X-ray Diffraction Powder Study on the Structure of the Antioxidant (+)-Catechin 4.5-Hydrate. *J. Am. Chem. Soc.* **2010**, *132*, 2928-2937. (l) Brouwer, D. H. NMR Crystallography of Zeolites: Refinement of an NMR solved Crystal Structure Using ab Initio Calculations of ^{29}Si Chemical Shift Tensors. *J. Magn. Reson.* **2008**, *194*, 136-146. (m) Brouwer, D. H.; Moudrakovski, I. L.; Darton, R. J.; Morris, R. E. Comparing Quantum-Chemical Calculation Methods for Structural Investigation of Zeolite Crystal Structures by Solid-State NMR Spectroscopy. *Magn. Reson. Chem.* **2010**, *48*, S113-S121. (n) Luchinat, C.; Parigi, G.; Ravera, E.; Rinaldelli, M. Solid-State NMR Crystallography through Paramagnetic Restraints. *J. Am. Chem. Soc.* **2012**,

134, 5006–5009.

3. Salager, E.; Stien, R. S.; Pickard, C. J.; Elens, B.; Emslay, L. Powder NMR Crystallography of Thymol. *Phys. Chem. Chem. Phys.* **2009**, *11*, 2610-2621.
4. Harper, J. K.; Grant, D. M. Enhancing Crystal-Structure Prediction with NMR Tensor Data *Cryst. Growth Des.* **2006**, *6*, 2315-2321.
5. (a) Harper, J. K.; Mulgrew, A. E.; Li, J. Y.; Barich, D. H.; Strobel, G. A.; Grant, D. M. Characterization of Stereochemistry and Molecular Conformation Using Solid-State NMR Tensors. *J. Am. Chem. Soc.* **2001**, *123*, 9837-9842. (b) Rienstra, C. M.; Tucker-Kellogg, L.; Jaroniec, C. P.; Hohwy, M.; Reif, M. T.; McMahon, B. T.; Lozano-Pe´rez, T.; Griffin, R. G. *De Novo* Determination of Peptide Structure with Solid-State Magic-Angle Spinning NMR Spectroscopy. *Proc. Natl. Acad. Sci. U.S.A.* **2002**, *99*, 10260-10265. (c) Castellani, F.; van Rossum, B.-J.; Diehl, A.; Schubert, M.; Oschkinat, H. Structure of a Protein Determined by Solid-State Magic-Angle-Spinning NMR Spectroscopy *Nature* **2002**, *420*, 98-102. (d) Harper, J. K.; Barich, D. H.; Hu, J.-Z.; Strobel, G. A.; Grant, D. M. Stereochemical Analysis by Solid-State NMR: Structural Predictions in Ambuic Acid. *J. Org. Chem.* **2003**, *68*, 4609-4614. (e) Jaroni, C. P.; MacPhee, C. E.; Bajaj, V. S.; McMahon, M. T.; Dobson, C. M.; Griffin, R. G. High-Resolution Molecular Structure of a Peptide in an Amyloid Fibril Determined by Magic Angle Spinning NMR Spectroscopy. *Proc. Natl. Acad. Sci. U.S.A.* **2004**, *101*, 711-716.
6. (a) Nieuwkoop, A. J.; Reinstra, C. M. Supramolcular Protein Structure Determination by Site-Specific Long-Range Intermolecular Solid State NMR Spectroscopy. *J.*

Am. Chem. Soc. **2010**, *132*, 7570-7571. (b) Bayro, M. J.; Debelouchina, G. T.; Eddy, M. T; Birkett, N. R.; MacPhee, C. E.; Rosay, M.; Maas, W. E.; Dobson, C. M.; Griffin, R. G. Intermolecular Structure Determination of Amyloid Fibrils with Magic-Angle Spinning and Dynamic Nuclear Polarization NMR. *J. Am. Chem. Soc.* **2011**, *133*, 13967-13974.

7. (a) Lange, A.; Schupp, T.; Petersen, F.; Carlomagno, T.; Baldus, M. High-Resolution Solid-State NMR structure of an Anticancer Agent. *ChemMedChem* **2007**, *2*, 522-527. (b) Heider, E. A.; Harper, J. K.; Grant, D. M. Structural Characterization of an Anhydrous Polymorph of Paclitaxel by Solid-State NMR. *Phys. Chem. Chem. Phys.* **9**, 6083-6097.

8. Bennett, A. E.; Reinstra, C. M.; Auger, M.; Lakshmi, K. V.; Griffen, R. G. Heteronuclear Decoupling in Rotating Solids. *J. Chem. Phys.* **1995**, *103*, 6951.

9. Pretsch, E.; Clerc, T.; Seibl, J.; Simon, W. *Tables of Spectral Data for Structural Determination of Organic Compounds*; Springer- Verlag: New York, 1989.

10. (a) Becke, A. D. Density Functional Thermochemistry. III. The Role of Exact Exchange. *J. Chem. Phys.* **1993**, *98*, 5648. (b) Lee, C.; Yang,W.; Parr, R. G. Development of the Colle-Salvetti Correlation-Energy Formula into a Functional of the Electron Density. *Phys. Rev. B* **1988**, *37*, 785-789.

11. Perdew, J. P.; Wang, Y. Accurate and Simple Analytic Representation of the Electron-Gas correlation Energy. *Phys. Rev. B* **1992**, *45*, 13244-13249.

12. Alderman, D. W.; Sherwood, M. H.; Grant, D. M. Comparing, Modeling, and Assigning Chemical-Shift Tensors in the Cartesian, Irreducible Spherical, and Icosahedral Representations. *J. Magn. Reson. Ser. A* **1993**, *101*, 188-197.

13. Harper, J. K.; Grant, D. M. Solid-State ^{13}C Chemical Shift Tensors in Terpenes. 3. Structural characterization of Polymorphous Verbenol. *J. Am. Chem. Soc.* **1999**, *122*, 3708 – 3714.

14. Stanek, J. Jr.; Moravcová, J.; Jary, J. Crystalline Methyl β–L_Rhamnofuranoside from Fisher Glycosidation of L-Rhamnose *J. Carb. Chem.* **1985**, *4*, 79-90.

15. Orendt, A. M.; Facelli, J. C. *NMR Crystallography*; Wiley: Chichester, 2009.

16. Alderman, D. W.; McGeorge, G.; Hu, J. Z.; Pugmire, R. J.; Grant, D. M. A Sensitive, High Resolution Magic Angle Turning Experiment for Measuring Chemical Shift Tensor Principal Values. *Mol. Phys.* **1998**, *95*, 1113-1126.

17. Johnston, J. C.; Iuliucci, R. J.; Facelli, J. C.; Fitzgerald, G.; Mueller, K. T. Intermolecular Shielding Contributions Studied by Modeling the ^{13}C Chemical Shift Tensors of Organic Single Crystals with Plane Waves. *J. Chem. Phys.* **2009**, *131*, 144503.

18. Liu, F.; Phung, C. G.; Alderman, D. W.; Grant, D. M. Carbon-13 Chemical Shift Tensors in meso-Erythritol, Measuring OH Dihedral Angles. *J. Am. Chem. Soc.* **1995**, *117*, 9323–9328.

19. Van Rossum, B. –J.; Steengaard, D. B.; Mulder, F. M.; Boender, G. J.; Schaffner, K.; Holzwarth, A. R.; de Groot, H. J. M. A Refined Model of the Chlorosomal Antennae of the Green Bacterium Chlorobium tepidum from Proton Chemical Shift Constraints Obtained with High-Field 2-D and 3-D MAS NMR Dipolar Correlation Spectroscopy. *Biochem.* **2001**, *40*, 1587-1595.

20. (a) Harris, R. K.; Cadars, S.; Emsley, L.; Yates, J.; Pickard, C. J.; Jetti, R. K. R.; Griesser, U. J. NMR Crystallography of Oxybuprocaine Hydrochloride,

Modification II. *Phys. Chem. Chem. Phys.* **2007**, *9*, 360-368. (b) Harper, J. K.; Strohmeier, M.; Grant, D. M. Pursuing Structure in Microcrystalline Solids with Independent Molecules in the Unit Cell using ^{1}H-^{13}C correlation data. *J. Magn. Reson.* **2007**, *189*, 20-31.

21. Cremer, D.; Pople, J. General Definition of Ring Puckering Coordinates. A. *J. Am. Chem. Soc.* **1975**, *97*, 1354–1358.

22. (a) Saenger, W.; Betzel, C. H.; Hingerty, B. E.; Brown, G. M. Flip-flop Hydrogen Bonding in a Partially Disordered System. *Nature*, **1982**, *296*, 581-583. (b) Steiner, T.; Mason, S. A.; Saenger, W. Topology of Cyclodextrin Inclusion Complexes. 27. Disordered Guest and Water Molecules, Three-Center and Flip-flop O–H···O Hydrogen Bonds in Crystalline β–Cyclodextrin Ethanol Octahydrate at T = 295 K: a Neutron and X-ray Diffraction Study. *J. Am. Chem. Soc.* **1991**, *113*, 5676-5687.